18. United States Environmental Protection Agency, *Test Method for Evaluating Solid Waste: Vol 1B*, EPA-SW-846, Washington DC, 1986.
19. APHA, AWWA and WEF, *Standard Method for the Examination of Water and Waste Water*, Washington DC, 2005, 21st edn.
20. Maliszewska-Kordybach, B., Polycyclic aromatic hydrocarbons in agricultural soils in Poland: preliminary proposals for criteria to evaluate the level of soil contamination. *Appl. Geochem*., 1996, **11**, 121–127.
21. Edwards, N. T., Polycyclic aromatic hydrocarbons (PAHs) in the terrestrial environment – a review. *J. Environ. Qual*., 1983, **12**, 427–441.
22. Yang, S. Y. N., Connell, D., Hawker, D. W. and Kayal, S. I., Polycyclic aromatic hydrocarbons in air, soil, and vegetation in the vicinity of an urban roadway. *Sci. Total Environ*., 1991, **102**, 229–240.
23. Koller, K., Brown, T., Spurgeon, A. and Levy, L., Recent development in low level exposure and intellectual impairment in children. *Environ. Health Perspect*., 2004, **112**, 987–994.
24. Martin, A. C., Rivero, V. C. and Marin, M. T. L., Contamination by heavy metal in soil in the neighborhood of a scrapyard of discarded vehicles. *Sci. Total Environ*., 1998, **212**, 145–152.
25. Bureau of Indian Standards, *Guidelines for the Quality of Irrigation Water*, Indian Standard Institute, New Delhi, 1986, pp. 116–124.

ACKNOWLEDGEMENTS. We thank the Ministry of Environment, Forest and Climate Change, Government of India, for funds (grant no. 19/32/2008-RE). We also thank Dr N. C. Talukdar (Director, Institute of Advanced Study in Sciences and Technology, Guwahati) for providing the necessary facilities to carry out the work.

Received 24 July 2015; revised accepted 14 March 2016

doi: 10.18520/cs/v110/i12/2285-2292

Measurement of tsunami wave eigenfunctions in deep, intermediate and shallower regions

Sudhir Kumar Chaturvedi[1,*], Ugur Guven[1] and Pankaj Kumar Srivastava[2]

[1]Department of Aerospace Engineering, and
[2]Department of Petroleum Engineering and Earth Sciences,
University of Petroleum and Energy Studies, Dehradun 248 007, India

The present communication describes a numerical study and investigation of the excitation of tsunami waves by an earthquake. Detailed analysis has been carried out to describe the properties of eigenfunctions which represent the values of wave potential, horizontal and vertical velocity, and acceleration components with angular frequencies corresponding to the deep, intermediate and shallow water waves. Analysis and measurement of eigenfunctions were also performed. It shows that as distance progresses from the deep to coastal regions, celerity reduces due to increment in significant wave heights. At 80 km distance from the origin of generation, celerity is 550 m/s in deep, 440 m/s in intermediate and 310 m/s in shallow water waves.

Keywords: Earthquake, eigenfunctions, simulation, tsunami.

TSUNAMI is a system of ocean gravity waves formed as a result of large-scale disturbance of the seabed[1]. It is a type of ocean waves normally seen on the beaches[2]. Tsunamis may be characterized in terms of their mode of generation, propagation, wavelength, time period, velocity and distribution from the distinct oceanic regions to the coastal areas for a particular region of interest. With the comparative studies, it has been studied that the wind generated waves show lesser impact on the coastline as compared to tsunami generated waves because of different wave characteristics such as wavelength and velocity of propagation[3,4]. Deep and mid-sea movements, which are free of coastal contamination, are vital for realistic tsunami forecasting and source identification with increased experience in tsunami analysis and simulated measurements[5]. The initial displacements of the free surface of different water wave conditions are induced by larger earthquakes of magnitude of more than 9.0 on the Richter scale, in which the generation of *N*-type waves is higher[6]. The dispersion relationship shows the better response of wavenumber variations with respect to bathymetery depths for each water wave conditions. It carries the significance role while the calculation of all properties[7].

Eigenfunctions are parameters involved in the study of distribution of wave motions with respect to variation of depth at a particular angular frequency of operation. The values of orbital velocity and distribution vary from deep to coastal waters[8]. Classification of deep and coastal water waves is made using correlations between depth and wavelength. If $d/L < 1/20$, it is known as shallow water condition, where d and L represent depth of ocean and wavelength respectively. If the ratio varies from 1/20 to 1/2, it is intermediate water condition[9]. If the ratio is more than 1/2, the region is considered as deep water. The impact at the coastal region is extremely high because a significant wave height increases due to less bathymetry as compared to the deep water[10]. Tsunami waves are known to shallow water waves. Airy wave theory is a linear theory for the propagation of waves on the surface of a potential flow and above a horizontal bottom. The free surface elevation $\eta(x, t)$ of one wave component is sinusoidal, as a function of horizontal position x and time t (refs 11–13), the eigenfunctions can be derived using the following relationships.

*For correspondence. (e-mail: sudhir.chaturvedi@ddn.upes.ac.in)

The surface generation for 2D waves (Figure 1) is given in eq. (1) (ref. 7)

$$\eta = a\cos(\omega t - kx). \tag{1}$$

This correlates the surface elevation (a), angular frequency (ω) and wavenumber ($k = 2\pi/L$) in time and space domain.

For deep water conditions, the wave potential function is given in eq. (2)

$$\phi = \frac{ga}{\omega} e^{-kz} \cos(\omega t - kx). \tag{2}$$

The dispersion relationship for wave conditions is expressed in correlation with bathymetry water depth, as given in eq. (3) (ref. 7)

$$\omega^2 = gk \tan h(kd), \tag{3}$$

where ω is the angular speed of the wave motion, k the wavenumber, $g = 9.81$ m/s^2 and d is the bathymetry depth. For deep water condition, eq. (3) can be represented as $\omega^2 = gk$, since $\tan h\,(kd) \simeq 1$.

The eigenfunctions along the x- and y-axis of the tsunami wave propagation are given in eqs (4)–(7)

$$u_x = \frac{\partial \phi}{\partial x} = \omega a e^{-kz} \sin(\omega t - kx), \tag{4}$$

$$u_z = \frac{\partial \phi}{\partial z} = \omega a e^{-kz} \cos(\omega t - kx), \tag{5}$$

$$a_x = \frac{\partial^2 \phi}{\partial^2 x} = \omega^2 a e^{-kz} \cos(kx - \omega t), \tag{6}$$

$$a_x = \frac{\partial^2 \phi}{\partial^2 z} = -\omega^2 a e^{-kz} \sin(kx - \omega t). \tag{7}$$

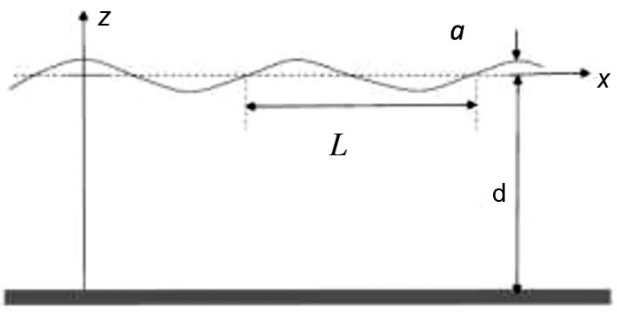

Figure 1. Wave representation in the ocean[15].

For intermediate water conditions, the mathematical equations for eigenfunctions are provided in eqs (8)–(12)

$$\phi = \frac{ga}{\omega} \frac{\cos h(kz + kd)}{\cos h(kd)} \cos(\omega t - kx), \tag{8}$$

$$u_x = \frac{\partial \phi}{\partial x} = \frac{\omega a \cos h(kz + kd)}{\sin h(kd)} \sin(\omega t - kx), \tag{9}$$

$$u_z = \frac{\partial \phi}{\partial z} = \frac{\omega a \sin h(kz + kd)}{\sin h(kd)} \cos(\omega t - kx), \tag{10}$$

$$a_x = \frac{\partial^2 \phi}{\partial^2 x} = \frac{\omega^2 a \cos h(kz + kd)}{\sin h(kd)} \sin(\omega t - kx), \tag{11}$$

$$a_z = \frac{\partial^2 \phi}{\partial^2 z} = -\frac{\omega^2 a \sin h(kz + kd)}{\sin h(kd)} \sin(\omega t - kx). \tag{12}$$

Similarly, the eigenfunctions for shallow water conditions are given in eqs (13)–(17)

$$\phi = \frac{ga}{\omega} \cos(\omega t - kx), \tag{13}$$

$$u_x = \frac{\partial \phi}{\partial x} = \frac{\omega a}{gd} \sin(\omega t - kx), \tag{14}$$

$$u_z = \frac{\partial \phi}{\partial z} = \frac{\omega a (d + z)}{d} \cos(\omega t - kx), \tag{15}$$

$$a_x = \frac{\partial^2 \phi}{\partial^2 x} = \frac{\omega^2 a}{kd} \cos(kx - \omega t), \tag{16}$$

$$a_x = \frac{\partial^2 \phi}{\partial^2 z} = \frac{\omega^2 a}{d} (d + z) \sin(kx - \omega t). \tag{17}$$

z is the vertical displacement of water perpendicular to the wave propagation.

The angular frequency for the shallow water waves is expressed as $\omega^2 = gd$.

The simulation work has been carried out using the bathymetry depth assumption of deep (8–9.8 km), intermediate (5–7 km) and shallow water (10 m to 1 km) waves respectively. The dispersion relationships have been applied to determine the respective wavelengths in each water wave condition. The wave heights for three conditions were assumed as 3, 6 and 10 m for deep, intermediate and shallow water waves respectively. This assumption depends on the simulation because in the

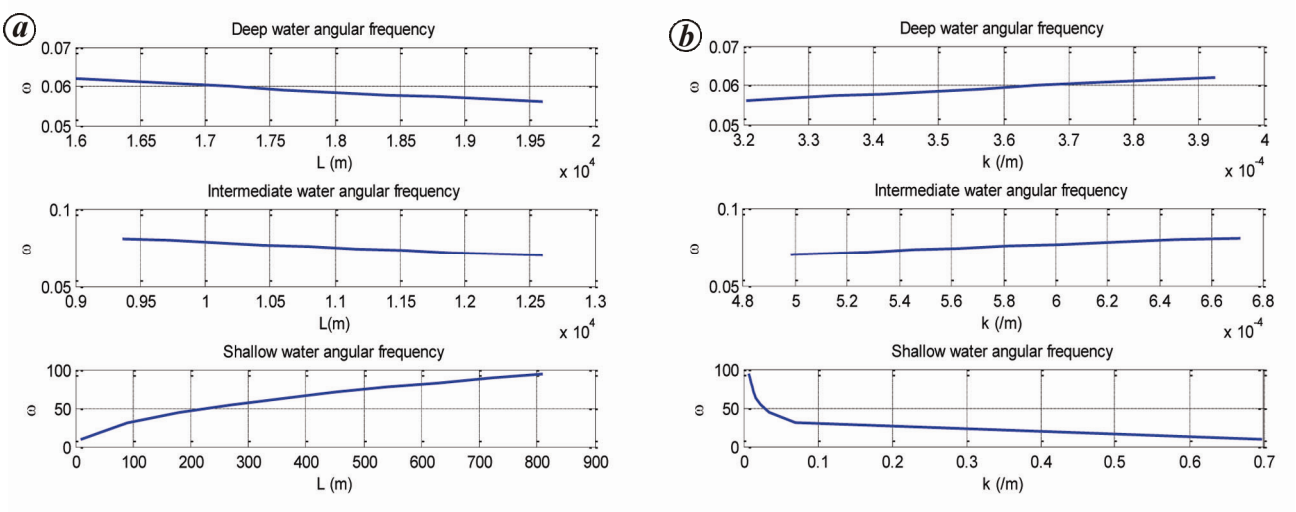

Figure 2. Angular frequency variation with respect to (***a***) wavelength and (***b***) wavenumber.

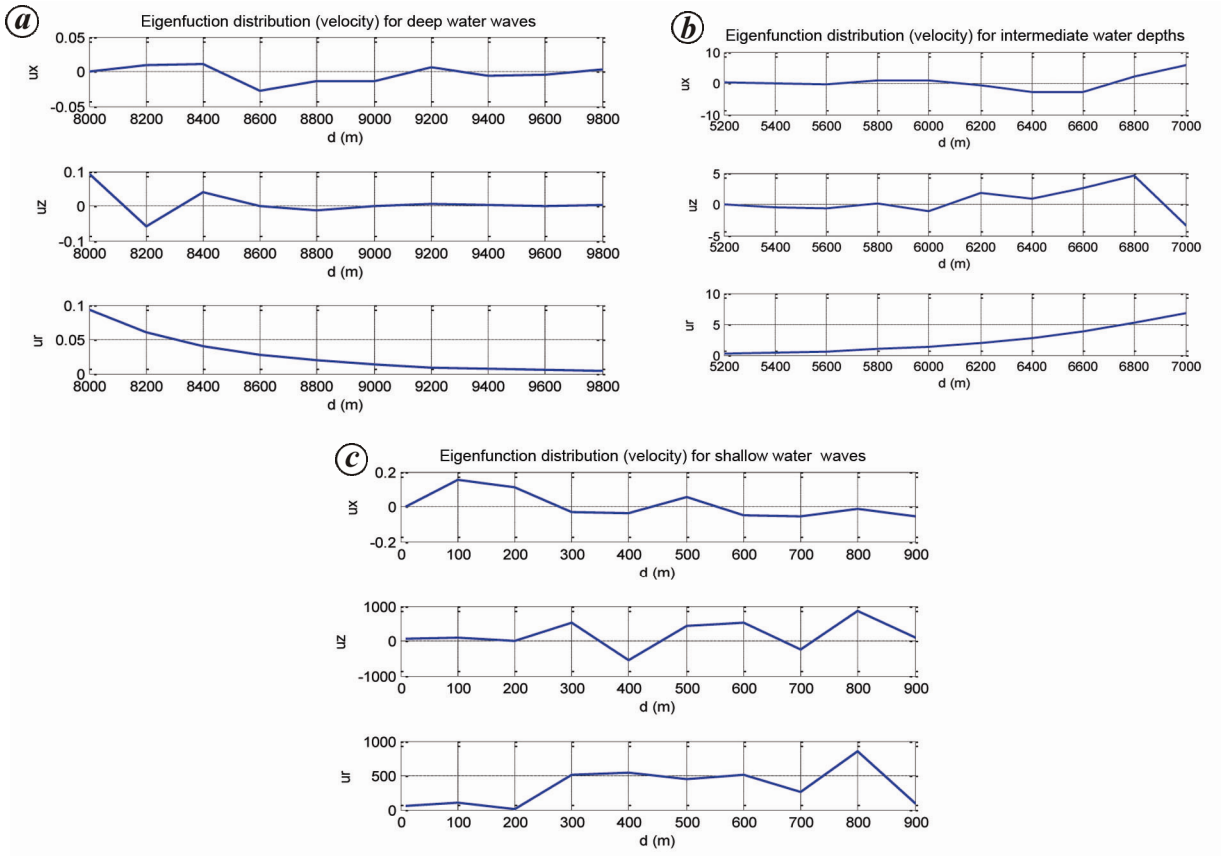

Figure 3. Eigenfunctions (velocity) for (***a***) deep, (***b***) intermediate and (***c***) shallow waters.

deep ocean, wavelength is large and wave height is less compared to the other water wave conditions[14].

Figure 2 shows the angular frequencies of all water waves. In deep waters, the wavelength is very large compared to the intermediate and shallow water waves. It can be concluded that the angular frequency shows decaying response in deep and intermediate waters compared to shallower water with respect to wavelength variation. Variation in ω is from 0.05 to 0.07 rad/s for deep, 0.05 to 0.1 rad/s for intermediate, and 0 to 100 rad/s for shallow waters. Furthermore, the right side of Figure 2 can also be described based upon the variation of angular

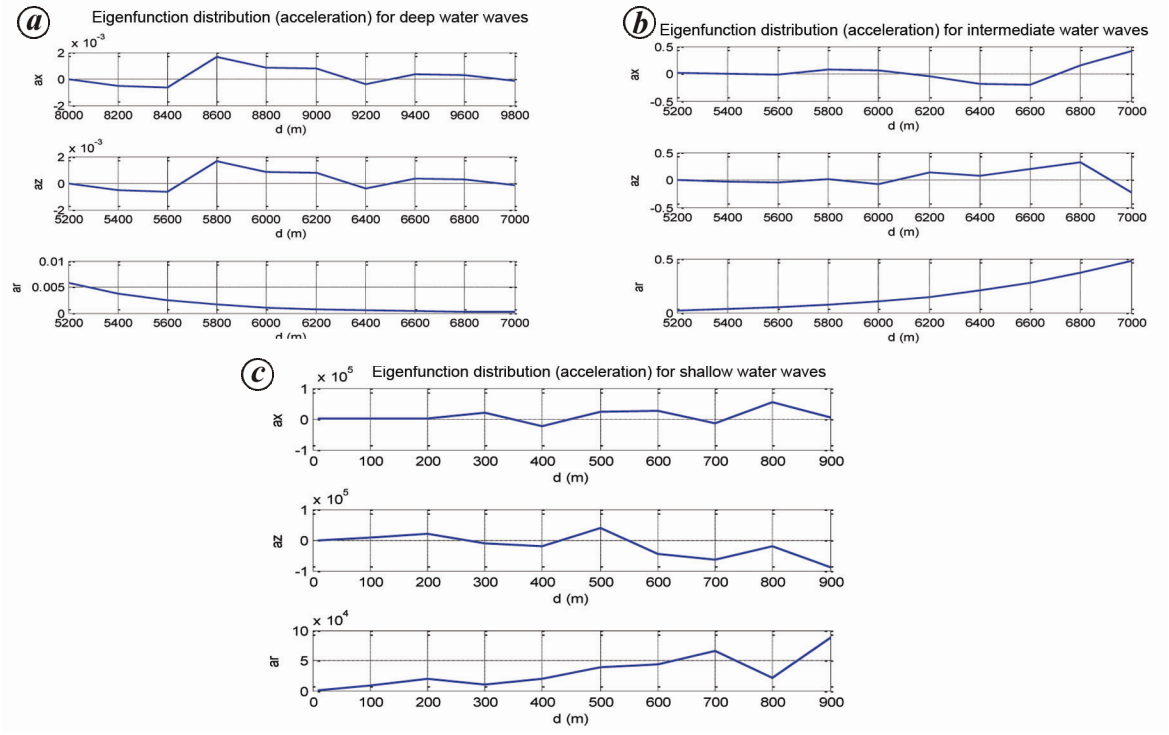

Figure 4. Eigenfunctions (acceleration) for (***a***) deep, (***b***) intermediate and (***c***) shallow waters.

frequency for deep and intermediate water waves. It can be clearly observed that, the value of angular frequency increases in deep water as compared to intermediate and shallow water due to the inverse relationship between k and L. It can also be concluded that in shallower water, the particles move with very high speed and the impact is more significant compared to the other two water wave conditions at a particular wave heights.

Figure 3 *a*–*c* shows the eigenfunctions in horizontal, vertical and resultant velocity components for all water wave conditions with respect to bathymetry depth. The resultant velocity in deep water varies from 0 to 0.1 m/s which is simulated at the depths of 8 to 9.8 km and in intermediate water, the result shows the increase in slope with the velocity variation from 0 to 10 m/s with reference to the depth of 5.2 to 7 km. In shallow water waves, the resultant velocity fluctuates from 0 to 1000 m/s at depths from 10 to 900 m. Analysis of the orbital acceleration has also been carried out (Figure 4 *a*–*c*). In deep water, the resultant acceleration is small and varies from 0 to 0.01 m/s^2 compared to the intermediate water, where the variation is from 0 to 0.5 m/s^2. The highest values of acceleration from 0 to 10×10^4 have been obtained in the shallow water waves.

From Figure 4 *c*, it can also be concluded that, the orbital acceleration at 900 m depth show a value of 9×10^4, hence the dynamic forces are very high approximately 1 km from the beaches. Once it is close to the beach, wave height increases whereas particle acceleration decreases because near the coast, due to geological structure of the earth's surface, inertia and gravity forces increase to the extreme limits, while particle acceleration and velocity values reach close to zero.

Figure 5 *a* and *b* represents variation of resultant eigenfunctions (velocity and acceleration) with respect to the time run-ups of the tsunami waves used under all water wave conditions. It shows nonlinear uniform response with respect to time because in deep and intermediate water waves, the decaying exponential factors as provided in equations (4)–(12). For shallow water waves, decay factor, orbital velocity and acceleration values do not depend on water depth. Figure 5 *c* shows the wave potential plot with respect to bathymetry depth for all water wave conditions. It can be seen that φ varies from –20 to +20 in case of the deep water, -2×10^4 to $+2 \times 10^4$ for intermediate water and –5 to +5 for shallower water conditions with respect to time. Figure 5 *d* presents results of celerity variation with respect to distance from the origin of tsunami waves for all water wave conditions. The results show that as tsunami waves progress from the deep to coastal regions, celerity reduces due to increment in significant wave heights. It can be seen that at 80 km distance from the origin of generation, the average celerity is as 550 m/s for deep, 440 m/s for intermediate and 310 m/s for shallow water respectively.

Measurements of the eigenfunction parameters correlated to tsunami waves run-ups have been carried out using Airy wave theory models for all water wave conditions. It has been observed in the present work that in deep waters, tsunami waves propagate with the higher

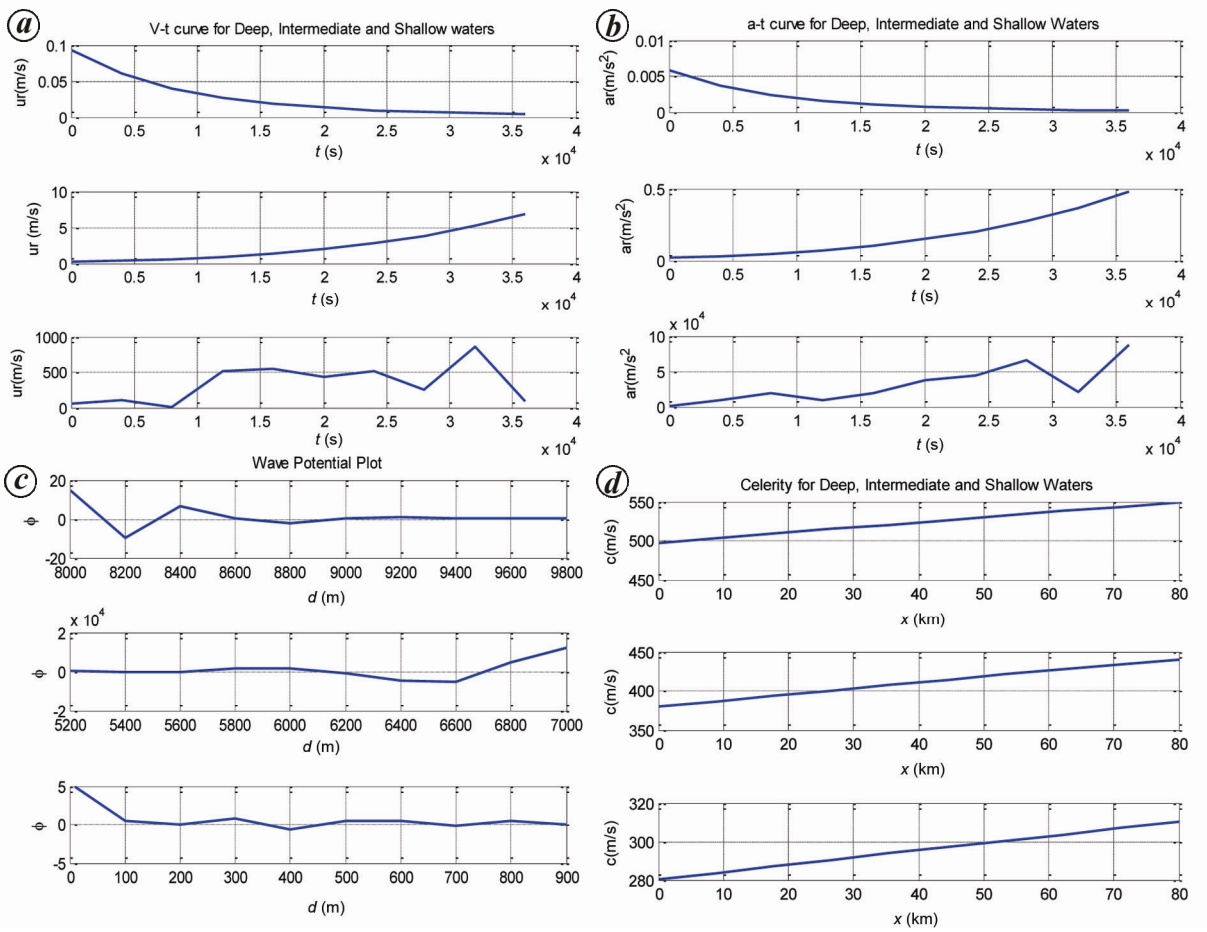

Figure 5. ***a***, Eigenfunction (velocity) with time; ***b***, eigenfunction (acceleration) with time; ***c***, wave potential with bathymetry depth; ***d***, celerity with distance.

velocity due to less angular frequency of orbital particles, while near the shorelines, particle movement is high, but linear velocity response diminishes. Using the dispersion relationships, celerity has been computed for all water wave conditions. In the shallow water region, celerity reduces and significant wave height increases. Tsunami with high energy amplitude causes high impact to the shoreline which results in extreme disaster.

1. Geist, E. L., Local tsunamis and earthquake source parameters. *Adv. Geophys.*, 1998, **39**, 117–209.
2. Princ, J. E., Characteristics of waves generated by local disturbance. *Trans. Am. Geophys. Union*, 1958, **39**, 865–874.
3. Zielinski, A. and Saxena, N., Rationale for measurement of midocean tsunami signature. *Mar. Geodesy*, 1983, **6**, 331–337.
4. Filloux, J. H., Bourdon tube deep sea tide gauges. In *Tsunamis in the Pacific Ocean*, University Press, Honolulu, 1970, pp. 223–238.
5. Josheph, A., *Tsunamis: Detection, Monitoring and Early-warning Technologies*, Academic Press, New York, USA, 2011.
6. Tadepalli, S. and Synolakis, C. E., The run-up of *N*-waves on sloping beaches. *Proc. R. Soc. London*, 1994, **445**, 99–112.
7. Dean, R. G., Evaluation and development of water wave theories for engineering application, Florida University, Special Report, Coastal Engineering Research Centre, U.S. Army, USA, 1974.
8. Eze, C. L. and Uko, D. E., Mathematical evaluation of tsunami propagation. *J. Appl. Sci.*, 2009, **4**, 213–216.
9. Massel, S. R., Furukawa, K. and Brinkman, R. M., Surface wave propagation in mangrove forests. *Fluid Dyn. Res.*, 1999, **24**, 219–249.
10. Craig, W. and Sulem, C., Numerical simulation of gravity waves. *J. Comput. Phys.*, 1993, **108**, 73–83.
11. Ward, S. N., Relationships of tsunami generation and an earthquake source. *J. Phys. Earth Sci.*, 1980, **28**, 441–474.
12. Dean, R. J. and Dalrymple, N. J., *Water Waves and Mechanics for Engineers and Scientists*, Prentice-Hall, Englewood Cliffs, NJ, 1984.
13. Okal, E. A., Seismic parameters controlling far-field tsunami amplitudes: a review. *Nat. Hazards*, 1988, **1**, 67–96.
14. Rick, S., *Introduction to Ocean Waves*, Scripps Institution of Oceanography, University of California, San Diego, USA, 1993.
15. Yeh, H., Design tsunami forces for onshore structures. *J. Disaster Res.*, 2007, **2**, 531–536.

ACKNOWLEDGEMENT. We thank the staff members of High computational lab, UPES, Dehradun for assisting in simulating the results. S.K.C. thanks his wife Sonam Chaturvedi for the help towards the documentation process.

Received 6 June 2015; revised accepted 2 March 2016

doi: 10.18520/cs/v110/i12/2292-2296